Biomedical Signal Processing and Control 79 (2023) 104087

Contents lists available at ScienceDirect

Biomedical Signal Processing and Control

journal homepage: www.elsevier.com/locate/bspc

ResDO-UNet: A deep residual network for accurate retinal vessel segmentation from fundus images

Yanhong Liu [a,b], Ji Shen [a,b], Lei Yang [a,b,*], Guibin Bian [a,c], Hongnian Yu [a,d]

[a] School of Electrical and Information Engineering, Zhengzhou University, Henan Province, 450001, China
[b] Robot Perception and Control Engineering Laboratory of Henan Province, 450001, China
[c] State Key Laboratory of Management and Control for Complex Systems, Institute of Automation, Chinese Academy of Sciences, Beijing 100190, China
[d] Built Environment, Edinburgh Napier University, Edinburgh EH10 5DT, UK

ARTICLE INFO

Keywords:
Retinal vessels segmentation
Deep learning
U-Net network
Residual DO-conv network

ABSTRACT

For the clinical diagnosis, it is essential to obtain accurate morphology data of retinal blood vessels from patients, and the morphology of retinal blood vessels can well help doctors to judge the patient's condition and give targeted therapeutic measures. Conventional manual retinal blood vessel segmentation by the doctors from the fundus images is time-consuming and laborious, while it also requires the rich doctor's expertise. With the strong context feature expression ability of deep convolutional neural networks (DCNN), it has shown a promising performance on retinal blood vessel segmentation, specially U-shape network (U-Net) and its variant. However, due to the information loss issue caused by multiple pooling operations and insufficient process issue of local context features by skip connections, most of segmentation methods still exist a certain shortcoming on accurate fine vessel detection. To address this issue, based on the encoder–decoder framework, a novel retinal vessel segmentation network, called ResDO-UNet, is proposed to provide an automatic and end-to-end detection scheme from fundus images. To enhance feature extraction capabilities, combined with depth-wise over-parameterized convolutional layer (DO-conv), a residual DO-conv (ResDO-conv) network is proposed to act as the backbone network to acquire strong context features. In addition, to reduce the effect of information loss caused by multiple pooling operations, taking advantages of max pooling and average pooling layers, a pooling fusion block (PFB) is proposed to realize nonlinear fusion pooling. Meanwhile, faced with insufficient process of local context features by skip connections, an attention fusion block (AFB) is proposed to realize effective multi-scale feature expression. Combined with the three public available data sets on retinal vessel segmentation, including DRIVE, STARE and CHASE_DB1, the proposed segmentation network could reach a state-of-the-art detection performance compared to other related advanced work.

1. Introduction

As an important part of the human body, retinal blood vessels undertake many critical functions. The morphological and density changes of retinal blood vessels are of quite important clinical significance, and it can be used as a key indicator of diagnostic disease development [1–4]. Vascular density measurement allows for more abundant information on the evaluation of blood flow, which can provide more objective indicators for the judgment of fundus blood flow, the changes in disease blood flow, and the follow-up of clinical diseases [5,6]. The fast development of imaging technology and clinical application have deepened the exploration of the diagnosis and treatment information and pathogenesis of the diseases, and the vascular density has been used for the diagnosis and disease monitoring of a variety of ophthalmic diseases. Accurate retinal vessel segmentation is the basis of the measurement of the vascular density, which is of great significance for clinical diagnosis. Therefore, the development of an accurate retinal vessel segmentation method is a basic and meaningful work.

Accurate retinal vessel segmentation is still a challenging task due to the fact that the fundus images are always against complex factors which will bring the great effect to the precise retinal blood vessel detection. (1) Complicated structures: The fundus images includes both thick retinal vessels and thin retinal vessels, which are both important for diagnosis and disease monitoring. And the detection precision of thin retinal vessels has a great effect to the whole detection precision. (2) Class imbalanced issue. Compared with background, the retinal vessels always occupy a smaller pixel portion in fundus images, which

* Corresponding author at: School of Electrical and Information Engineering, Zhengzhou University, Henan Province, 450001, China.
E-mail address: leiyang2019@zzu.edu.cn (L. Yang).

https://doi.org/10.1016/j.bspc.2022.104087
Received 27 January 2022; Received in revised form 18 June 2022; Accepted 8 August 2022
Available online 19 August 2022

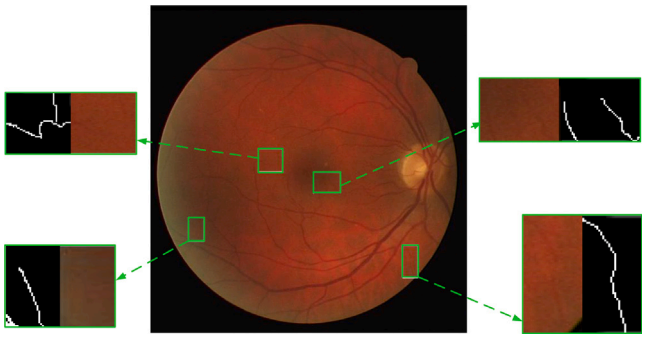

Fig. 1. Details of local image patches in retinal fundus images.

causes serious class imbalance issue to bring a ceratin challenge to accurate retinal vessel segmentation. (3) Poor image quality. The fundus images are against other complex factors to cause poor image quality, such as, low contrast, uneven illumination, etc. Fig. 1 shows some sample patches from fundus images, and they present the issue of poor image quality, such as low contrast, uneven illumination, weak texture, which make the retinal vessels difficult to be recognized.

To obtain the morphological changes of retinal blood vessels, various attempts have been proposed and improved to enhance the detection abilities. During the initial stage, it was generally marked manually by medical personnel of relevant disciplines, which was very labor-consuming and had a certain requirements for the professional quality of medical personnel. In order to reduce the pressure of doctors and reduce the errors caused by manual labeling, due to the success of computer vision, much model-based methods have been applied into the image analysis of fundus images combined with image processing operators. Joarse et al. proposed an automatic retinal blood vessel segmentation method, which used the two-dimensional (2D) Gabor and digital image processing method to extract retinal blood vessels [7]. To solve the problem that the traditional matched filtering could not effectively identify non-vascular pixels, Zhang et al. proposed an improved matched filtering model, which detected retinal blood vessels according to the response of fundus images by combining the original matched filtering and the first-order gaussian derivative which had achieved good results in the early research of vascular segmentation [8]. Roychowdhury et al. proposed a retinal vessel segmentation method based on gaussian mixture model to extract retinal blood vessels from fundus images [9]. Through the manual designed detection laws for the retinal blood vessels, the model-based methods do not need too much training data, and have higher computational efficiency. However, the design of detection laws always relies on the expert experience, and much repeated attempts.

In recent years, with the rapid improvement of high-performance hardware and big data, the deep learning has got fast development due to strong context feature expression ability [10]. It could well process the raw data and realize automatic feature expression to provide an end-to-end detection scheme, such as object classification [11], object detection [12], image segmentation [13]. Due to the success of DCNNs, much segmentation networks have been proposed to apply into the field of medical images, such as full convolution neural network (FCN) [14], DeepLab [15], SegNet [16], U-Net [17], etc. Through the introduced skip connections, the U-Net network could effectively merge low-level and high-level image features to reduce the semantic gap issue, which has shown a promising detection ability on medical images [18,19]. Alom et al. proposed a R2U-Net model for medical image segmentation, which used the recurrent convolution to replace the traditional convolution to ensure better feature representation [20]. To address the class imbalanced issue, Guo et al. proposed a SA-Net model for retinal vessel segmentation by adding a spatial attention block to acquire the discriminative features about retinal vessels [21]. To optimize the skip connections, combined with Bi-Directional ConvLSTM block, Azad et al. proposed a Bi-directional ConvLSTM U-Net network for medical image segmentation to capture more discriminative information [22]. Due to the success of U-Net network on medical image segmentation, it is set as the baseline network of the proposed ResDO-UNet network for retinal vessel segmentation.

To enhance the segmentation performance of U-Net network, many variants have been proposed to enhance the segmentation performance. Oktay et al. proposed an attention U-Net network to make the segmentation network to emphasize the micro objects or details [23]. On the basis of U-Net network, Zhang et al. proposed a boundary enhancement and feature denoising module (BEFD) to replace the skip connections to enhance the ability of boundary segmentation and reduce the effect of image noise in the low-level feature maps [24]. In addition, sobel edge detection algorithm was also introduced to obtain additional edge prior information. To improve the segmentation ability of backbone network, combined with generative adversarial network, Lin et al. proposed an improved U-Net network with generative adversarial training to acquire an effective backbone network for retinal vessel segmentation [25]. Faced with variable vessels, due to different feature representation abilities of different network layers, Lu et al. proposed a cascaded segmentation network based on feature fusion, called termed LF-UNet, for retinal layer segmentation [26]. To acquire the temporal modeling information, Li et al. proposed a CR-UNet network based on recurrent neural networks for ultrasound image segmentation [27]. Combined with a spatial attention block and channel attention block, Mou et al. proposed a CS2 network for medical image segmentation, which had shown a better segmentation performance on 2D and three-dimensional (3D) images [28]. Although the U-Net network and its variant networks have proven good segmentation performance on retinal vessel segmentation, they still exist a certain shortcoming on precise image segmentation due to some shortcomings, such as the information loss issue, insufficient process issue of local context features, etc.

Combined with the above analysis, a novel retinal vessel segmentation network, called ResDO-UNet, is proposed to provide an automatic and end-to-end vessel segmentation scheme from fundus images. Experimental results on multiple public data sets about retinal vessel segmentation prove the superiority of proposed ResDO-UNet network compared with other advanced segmentation networks. The main contributions of this paper are as follows.

(1) A novel deep segmentation network, called ResDO-UNet, is proposed for automatic and accurate retinal vessel detection.

(2) A ResDO-conv network is proposed to act as the backbone network to acquire strong context features.

(3) To reduce the effect of information loss caused by multiple pooling operations, a PFB network block is proposed to realize nonlinear fusion pooling.

(4) Aimed at insufficient process issue of local contextual features by skip connections, an AFB network block is proposed to realize effective multi-scale feature expression.

The remaining part of this paper is organized as follows. Section 2 gives the detailed description about the proposed ResDO-UNet network. Section 3 describes the experimental data sets and data preprocessing method. Section 4 provides the related experimental configuration, and special experimental results and analysis. The conclusions and prospect of this paper are given in Section 5.

2. Proposed method

To address the segmentation tasks of retinal blood vessels, a novel ResDO-UNet network is proposed to realize automatic vessel segmentation from fundus images. This section gives the detailed description about the whole network framework of proposed ResDO-UNet network and each network block.

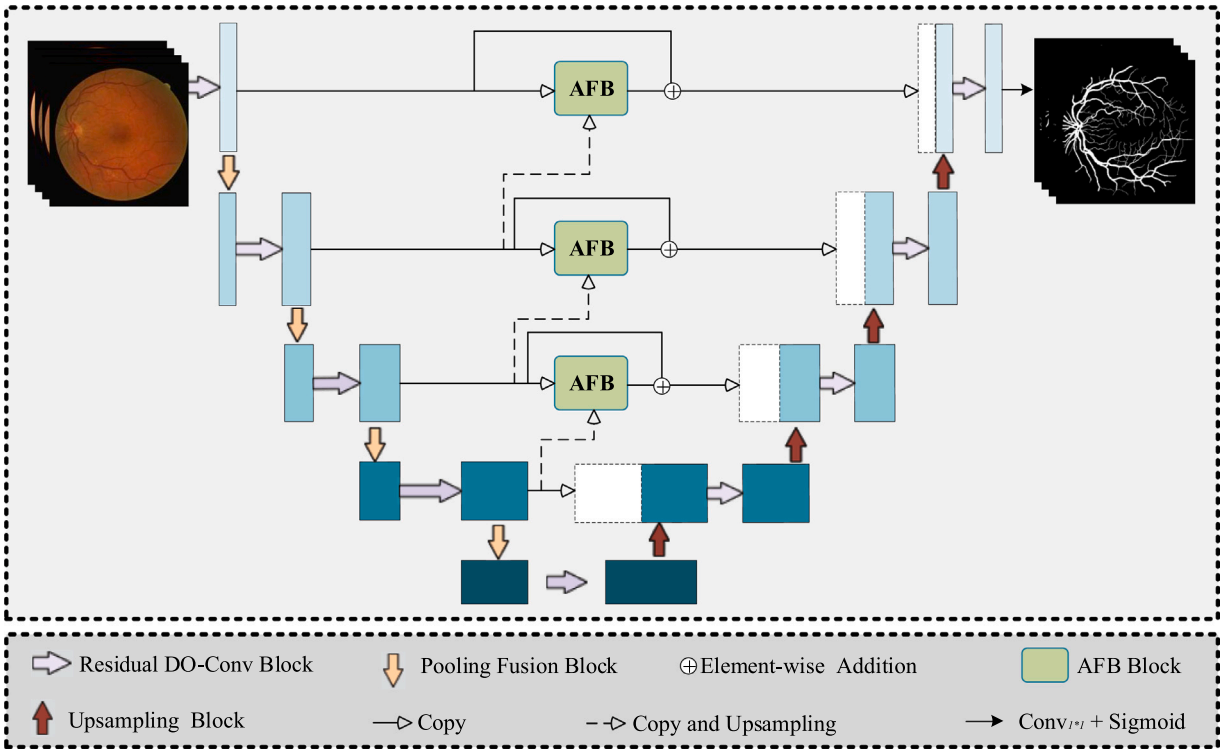

Fig. 2. Network structure of the proposed ResDO-UNet network.

Table 1
Abbreviation list in this paper.

Case	Words	Abbreviations
1	Batch Normalization	BN
2	Rectified Linear Unit	ReLU
3	Atrous Spatial Pyramid Pooling	ASPP
4	Sensitivity	S_e
5	Specificity	S_p
6	Accuracy	A_{cc}
7	Binary Cross Entropy	BCE
8	Squeeze-and-Excitation	SE
9	Contrast Limited Adaptive Histogram Equalization	CLAHE

2.1. Word abbreviation

For better reading about this paper, the abbreviations about common words are given in this paper, and Table 1 gives the special the full words and the corresponding abbreviations about common words.

2.2. Network structure

Fig. 2 shows the whole network structure of proposed ResDO-UNet network. It could be divided into two parts: backbone network and attention fusion block. To realize effective context feature representation, taking with the encoder–decoder framework, a ResDO-conv network is built to act as the backbone network. Faced with the information loss issue caused by multiple pooling operations, a PFB network block is proposed to integrate into the ResDO-conv network to provide a reasonable and nonlinear downsampling process to retain as much information as possible. Aimed at insufficient process issue of local context features, an AFB network block is proposed to optimize the raw skip connections for effective multi-scale feature expression.

2.3. Backbone block

An effective backbone network is the premise for accurate retinal vessel segmentation. As a basic and core building block, the convolutional layer [29] has been widely used in the field of deep learning due to its powerful feature extraction capabilities. The feature extraction ability of the convolution layer is associated with the detection performance of the entire backbone network.

DO-Conv layer could enhance the convolutional layer via additional depth-wise convolution, where each input channel is converted using a different 2D kernel [30]. Meanwhile, the DO-Conv layer does not increase the computational complexity which could provide an effective mean for performance optimization of DCNNs. To augment the convolutional layer, the DO-conv layer is proposed in this paper to act as the basic component of proposed ResDO-UNet network.

The residual block provides an effective mechanism for learning a diverse set of feature maps [31]. Due to the advantage of residual block, combined with the DO-conv layer, a ResDO-conv network block is built to construct the backbone network, as shown in Fig. 3. Each DO-conv layer follows by a BN layer and a ReLU function. Here, the 1*1 convolutional layer is introduced to adjust the channel number of feature maps.

Combined with the ResDO-conv network block, it is used to construct the encoder block and decoder block of backbone network. The encoder block is used for feature encoding of raw images to acquire multi-scale context features. Each unit in encoder block includes a ResDO-conv network block and a PFB block.

And the decoder block is used to restore the information of segmented objects from the encoding feature maps. Accordingly, each unit in decoder block includes a ResDO-conv network block and upsampling layer.

Meanwhile, to avoid the semantic gap issue, the skip connections are also introduced to merge low-level image features from encoder unit and high-level image features from decoder unit.

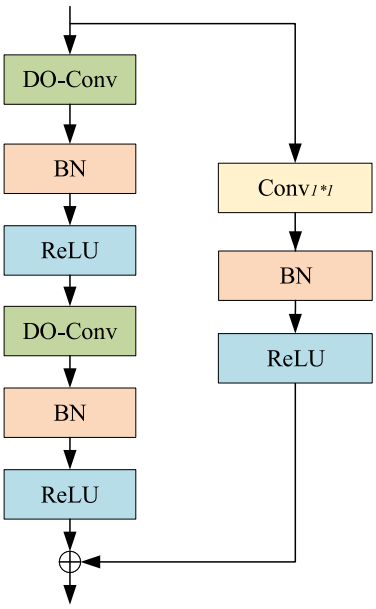

Fig. 3. Network structure of ResDO-conv network block.

2.4. Pooling fusion block

The pooling process is an important part of DCNNs for feature downsampling [32]. Combined with a series of convolution and pooling operations, more abstract context features could be acquired. However, with the increase of network layers, the feature information on micro objects or details also will be lost to affect the detection precision of thin retinal vessels.

To reduced the effect of information loss issue caused by multiple pooling operations, a PFB network block is proposed to realize nonlinear fusion pooling and acquire more context features. Fig. 4 gives the special network structure of proposed PFB block.

To take advantages of different pooling functions, the average pooling layer and the maxpooling layer are separately adopted for feature downsampling. And the downsampled 2D feature maps are concatenated together for information fusion to detect more context features. Meanwhile, the fusion features are fed into a 1*1 convolutional layer to adjust the channel number of feature maps.

2.5. Attention fusion block

For the typical U-Net network, to avoid the semantic gap issue, the skip connections are also introduced to merge low-level and high-level image features. However, it is a native method which will cause insufficient process issue of local context features. Meanwhile, due to limited receptive fields, it also has a certain shortcoming on multi-scale feature representation. To address these issues, an AFB network block is proposed to optimize the raw skip connections for effective multi-scale feature expression.

Faced with multi-scale feature expression, the convolution layers with large kernel sizes are always introduced to acquire large receptive fields. Combined with the convolution layers with different kernel sizes, different receptive fields could be acquired for multi-scale feature representation [33]. However, the convolution layers with large kernel sizes will bring a large of calculation cost to affect the computational efficiency. The ASPP block provides an effective means for multi-scale feature expression, which could well acquire different receptive fields through convolution layer with different expansion rates [34]. Combined with the advantages of ASPP block, an attention fusion block is proposed in this paper (see Fig. 5).

Table 2
Specifications about public retinal vessels segmentation sets.

Data set	Number of images	Train/Test	Image resolution
DRIVE	40	20/20	584*565
CHASE_DB1	28	20/8	999*960
STARE	20	15/5	700*605

To acquire more context information, the lower-level and higher-level feature maps are concatenated together to feed into the attention fusion block. Especially, the bilinear interpolation is applied into higher-level feature maps to keep the same size with the lower-level feature maps. On the basis of dilated convolutions [35], three network branches with different dilated rates are built to acquire different receptive fields. Here, the dilation rates for these three branches are set as 1, 2, 4. And the output feature maps are concatenated together for multi-scale feature representation.

To capture more discriminative information, an attention block is proposed to realize channel calibration of multi-channel feature maps. The SE block is a typical channel attention block and could capture the importance of each channel, which has proven good optimization performance on different DCNNs [36]. It could be easily integrated to any network model to enhance the detection ability. Due to the success of SE block, it is adopted to apply into the multi-channel feature maps to highlight important channels. The channels with significant semantic information are weighted higher to make it easy detected. And a 1×1 convolution layer is adopted to perform the channel compression.

3. Experiment data and preprocessing

To better verify the segmentation performance of proposed ResDO-UNet network, the suitable data sets are the basis for model evaluation and comparison. Here, three public data sets about retinal vessel segmentation are adopted in this paper for experiment analysis. This section gives the details about the data sets and corresponding image preprocessing method.

3.1. Data set

To fully evaluate and test the segmentation performance of proposed ResDO-UNet network. Here, three common public data sets about retinal vessel segmentation are adopted in the related segmentation experiments, including DRIVE set, CHASE_DB1 set, and STARE set.

DRIVE Set: As a common data set for retinal vessel segmentation, the DRIVE set contains 40 color images with 3 channels, and the image size of each image is 584 * 565 pixels with three channel [37]. For the model training and test, it is divided into two parts with a ratio of 1:1: training set and test set. 20 images are for training and the remaining part is used for model test. At the same time, this data set also provides a circular field of view mask for each image to facilitate the performance evaluation.

CHASE_DB1 Set: It is collected from the left and right eyes of school children, which includes 28 color fundus images with 999*960 image size [38]. Each image is annotated by two independent human experts. Here, 20 images are used for network training and 8 images are used for network test.

STARE Set: The STARE set includes 20 color fundus images with 3 channels contained manually labeled segmentation masks from human experts [7]. The image size of each image is 700*605. To serve the model training and test, 15 images are selected as the training images and the remaining images are adopted as test images. Fig. 6 gives the sample images from these data sets. Table 2 gives the special details about these data sets.

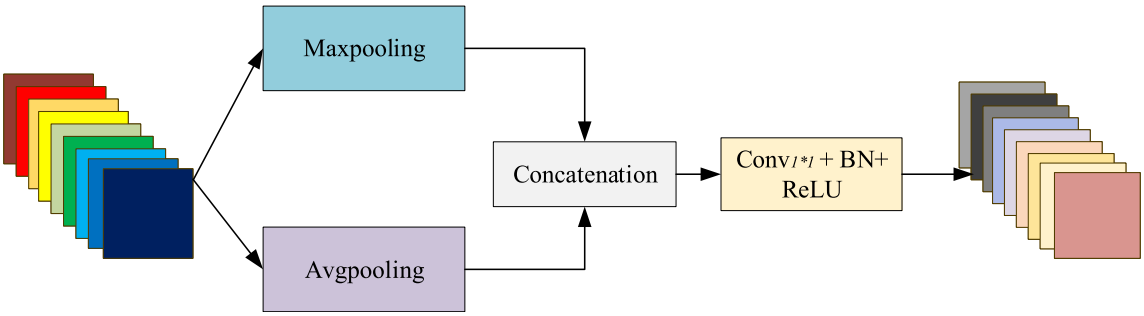

Fig. 4. Network structure of proposed PFB network block.

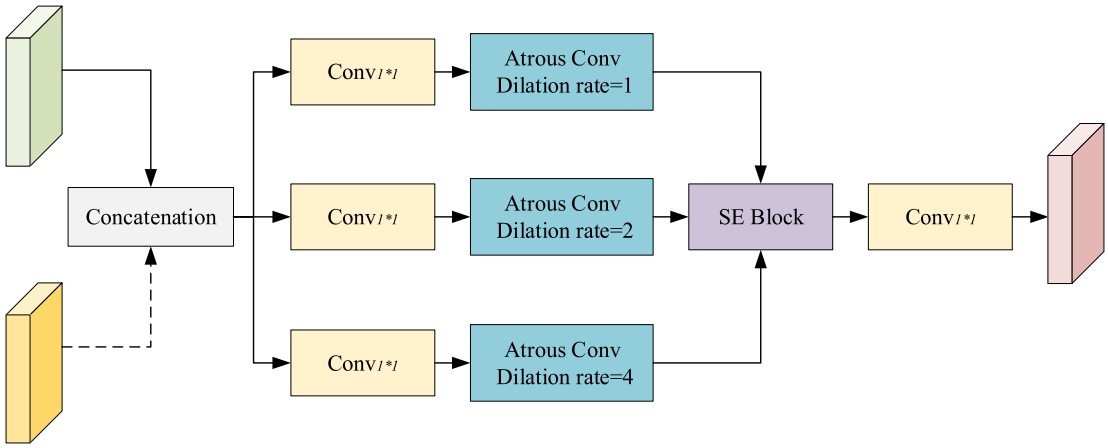

Fig. 5. Network structure of AFB block.

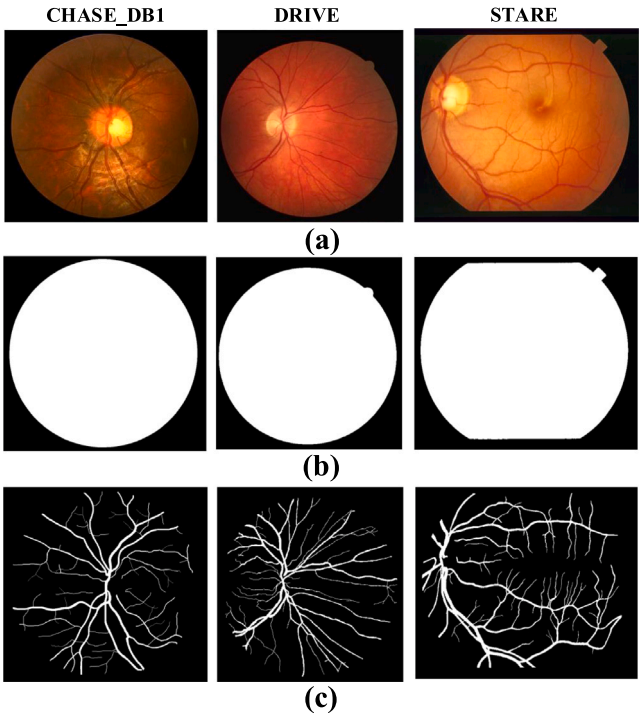

Fig. 6. Examples from three databases. The first row is the original images, middle row is the corresponding masks, and last row is the corresponding ground truth.

3.2. Image preprocessing

On the basis of raw images, conventional image processing methods are adopted to generate some new samples for model training, such as image graying, image normalization, CLAHE transformation and gamma correction. Fig. 7 shows the sample image with image preprocessing.

As shown in Fig. 7, it could be seen that the imbalance phenomenon between light and dark areas has been improved with image preprocessing. And the pixel contrast of the blood vessels has been enhanced.

3.3. Image crop

The model training of DCNNs always relies on large-scale data set. Therefore, these small-scale data sets could be directly applied into the model training. To better serve the model training of proposed segmentation network, the image crop is proposed to apply into each data set for data augmentation.

The random image crop is performed on the fundus images in training set to generate much image patches with 48*48. Here, for the DRIVE set, CHASE_DB1 set, and STARE set, 200,000, 250,000 and 250,000 image patches are extracted respectively from the training sets. Here, 10% is used to as the validation set. Especially, the images in test set are cropped sequentially for performance visualization. Fig. 8 shows the sample image patches.

4. Experiment results and analysis

To better show the superiority of proposed ResDO-UNet network, the qualitative analysis and quantitative analysis are introduced for performance evaluation.

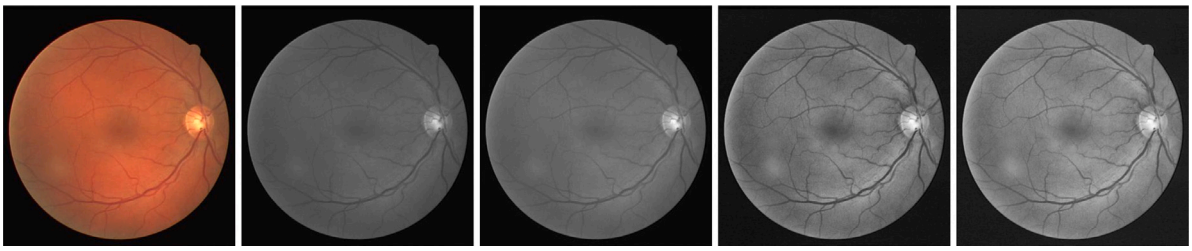

Fig. 7. Examples of image preprocessing. From left to right, these images separately indicate raw images, image graying, image normalization, CLAHE transformation, gamma correction.

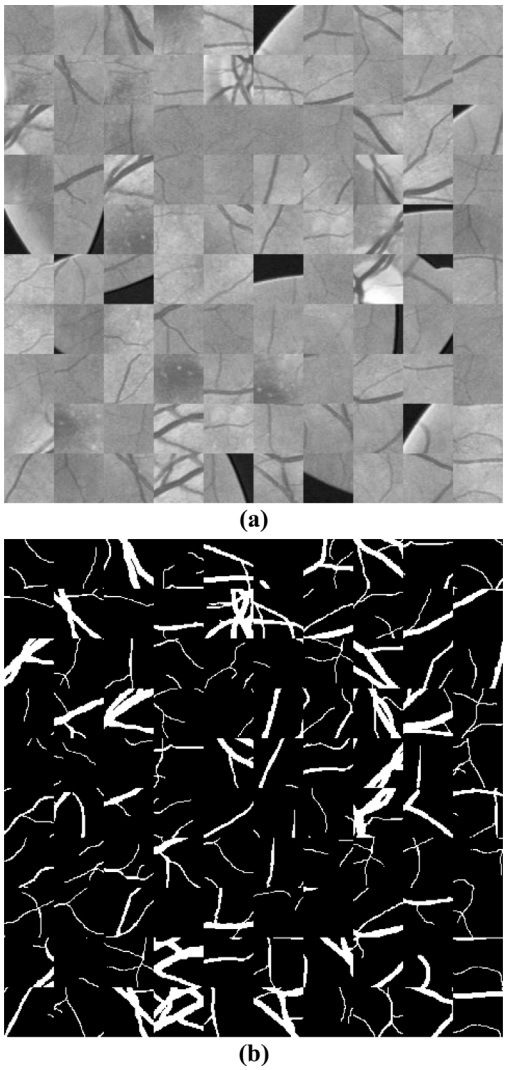

Fig. 8. Example image patches. (a). Raw image patches; (b). Corresponding ground truth.

Firstly, the special network configuration and related evaluation indicators are given. Secondly, the ablation study and comparative research is adopted to analysis the segmentation performance of proposed ResDO-UNet network. Finally, the qualitative analysis is given to more intuitively observe the segmentation effect.

4.1. Evaluation metrics

In order to quantify the segmentation performance of different networks comprehensively, some evaluation metrics are adopted to evaluate the segmentation ability which are commonly used in medical image segmentation, including S_e, S_p, A_{cc} and F_1 score.

(1) S_e: It represents the proportion of pixels correctly classified objects (see Eq. (1)), and it is used to measure the correctly classified blood vessels.

$$S_e = \frac{TP}{TP + FN} \tag{1}$$

where TP, TN, FP, and FN respectively represent True Positive, True Negative, False Positives, and False Negatives.

(2) S_p: Fundus vascular segmentation is a binary semantic segmentation task. It measures the proportion of pixels correctly classified for background, as Eq. (2).

$$S_p = \frac{TN}{TN + FP} \tag{2}$$

(3) A_{cc}: It reflects the proportion of the correct number of pixel classification in the total number of pixels, as Eq. (3).

$$A_{cc} = \frac{TP + TN}{TP + FP + TN + FN} \tag{3}$$

(4) F_1 score: F_1 can reflect the precision of binary classification model in the case of class imbalanced issue. The definition of F_1 is as Eq. (4).

$$F_1 = \frac{2 * TP}{2 * TP + FP + FN} \tag{4}$$

4.2. Experimental configuration

For the proposed ResDO-UNet network, it is built with the PyTorch framework.[1] To speed up the model training and evaluation, all segmentation experiments are performed on the NVIDIA Geforce RTX-3090 GPU platform with 24 GB memory.

For the model training, the overall training epoch is set to 50, and the early stopping epoch is set to 5 to prevent over fitting. The learning rate was set to 0.01, and the batch size is set as 64. Due to the advantage of BCE loss on binary classification, the BCE loss is adopted to act as the loss function (see Eq. (5)).

$$L = -\frac{1}{N}\sum_{1}^{N}[g_i \log(p_i) + (1 - g_i)\log(1 - p_i)] \tag{5}$$

where g_i indicates the ground truth of sample i. g_i is 1 if the instance belongs to the positive class, and g_i is 0 otherwise. p_i indicates the corresponding predicted values. N indicates the sample numbers.

Here, the Adam optimizer is selected to guide the network training. Especially, for these three public data sets, the related segmentation experiments are also with the same network configurations. To make a fair experiment comparison, the 3-fold cross-validation was performed in our segmentation experiments for better performance evaluation.

[1] PyTorch: https://pytorch.org/.

Table 3
Experiment results of ablation study.

Data set	ResDO-conv block	AFB block	PFB block	S_e	S_p	A_{cc}	F_1
DRIVE	×	×	×	0.7737	0.9785	0.9537	0.8192
DRIVE	✓	×	×	0.7786	0.9780	0.9534	0.8200
DRIVE	✓	✓	×	0.7946	0.9789	0.9555	0.8197
DRIVE	✓	✓	✓	**0.7985**	**0.9791**	**0.9561**	**0.8229**
CHASE_DB1	×	×	×	0.7834	0.9794	0.9665	0.8192
CHASE_DB1	✓	×	×	0.7851	0.9815	0.9634	0.8221
CHASE_DB1	✓	✓	×	0.7936	**0.9818**	0.9629	0.8111
CHASE_DB1	✓	✓	✓	**0.8020**	0.9794	**0.9672**	**0.8236**
STARE	×	×	×	0.7737	0.9837	0.9632	0.8301
STARE	✓	×	×	0.7773	**0.9872**	0.9634	0.8277
STARE	✓	✓	×	0.7858	0.9827	0.9598	0.8184
STARE	✓	✓	✓	**0.8039**	0.9836	**0.9635**	**0.8315**

4.3. Ablation study

In order to observe the impact of each module proposed in this paper on the actual segmentation performance, the ablation study is adopted to test each network block. Here, a four-layer U-Net model is set as the baseline network. Combined with the different network blocks, including ResDO-conv block, AFB block and PFB block, the proposed ResDO-UNet networks with different network configurations are built for ablation analysis. Table 3 gives the special experiment results of ablation study.

Combined with the ablation results in Table 3, it can be seen that after adding these network modules, the segmentation performance of proposed ResDO-UNet network on the three public data sets has improved compared with the backbone network.

For the DRIVE set, the proposed ResDO-UNet network has reached 0.9561, 0.7985, 0.9791 and 0.8229 on A_{cc}, S_e, S_p and F_1 score respectively. The S_e indicator gets the most obvious improvement among them, from 0.7737 to 0.7985, which mainly comes from the contribution of proposed AFB block. When the AFB block is added, S_e has got increased from 0.7786 to 0.7946. At the same time, S_p and F_1 also increased slightly, reaching 0.9791 and 0.8229 respectively.

The proposed network blocks also have acquired a better performance enhancement on the CHASE_DB1 set. Although the S_p does not get improved, the key indicators (A_{cc}, S_e and $F1$ score)) get significant improvement. Among them, the S_e also gets significantly improved, and it could reach up to 0.8020, which is higher than that of backbone network.

Like to the CHASE_DB1 set, the proposed ResDO-UNet network has acquired a similar phenomenon. Except for the S_p, with the introduced network blocks, other evaluation indicators also have been improved. And S_e gets increased from 0.7737 to 0.8039, which indicates a better segmentation ability on details.

Combined with the above ablation experimental results, it could well prove the effectiveness of proposed network blocks to the performance improvement of proposed ResDO-UNet network.

4.4. Comparison with other advanced models

To better show the superiority of proposed ResDO-UNet network, some advanced segmentation models performed on these data sets are selected to set as the comparative experiments. Combined with the introduced evaluation indicators, Table 4- Table 6 gives the special experimental results of different segmentation models on DRIVE set, CHASE_DB1 set, and STARE set.

As shown in Table 4, the proposed ResDO-UNet network could reach up to 0.7985 on S_e and 0.8229 on F_1 score, which are higher than other segmentation models. Compared with the best results from other comparative networks, the numerical difference between S_p and A_{cc} is 0.0066 and 0.0124, which does not cause significant decline.

For the STARE set in Table 5, the proposed ResDO-UNet network still achieved the best results in S_e and F_1 score, with the values of 0.7963 and 0.8172. It could reach up to 0.9792 on S_p, and 0.9567 on A_{cc}. Referring to the best results by other comparative networks, S_p has a numerical gap of 0.0109 and A_{cc} has a numerical gap of 0.027.

On the CHASEDB1 set, taking with comparative results in Table 6, the proposed ResDO-UNet network could reach up to 0.8020, 0.9794, 0.9672 and 0.8236 on S_e, S_p, A_{cc} and F_1 score respectively. Compared with the segmentation results from other comparative networks, it also acquires the highest values on A_{cc} and F_1 score.

Combined with the above experimental results, the proposed ResDO-UNet network both could the highest values of S_e and F_1 score on DRIVE, CHASE_DB1, and STARE sets, but the improvement effects

Table 4
The comparative results for different segmentation methods on DRIVE data set.

Method	Year	S_e	S_p	A_{cc}	F_1
Li et al. [39].	2015	0.7569	0.9816	0.9527	–
Roychowdhury et al. [40].	2015	0.7249	0.9830	0.9620	–
Liskowski et al. [41].	2016	0.7811	0.9807	0.9535	–
Orlando et al. [42].	2016	0.7897	0.9684	–	0.7857
Mo et al. [43].	2017	0.7779	0.9780	0.9521	–
Alom et al. [20].	2018	0.7792	0.9813	0.9556	0.8171
Zhuang et al. [44].	2018	0.7856	0.9810	0.9561	0.8202
Yan et al. [45].	2018	0.7653	0.9818	0.9542	–
Xia et al. [46].	2018	0.7979	**0.9857**	**0.9685**	–
Yan et al. [47].	2019	0.7631	0.9820	0.9538	–
Guo et al. [48].	2019	0.7891	0.9848	0.9674	–
Lops et al. [49].	2019	0.7903	0.9813	0.9567	–
Yin et al. [50].	2020	0.7614	0.9837	0.9604	–
Adarsh et al. [51].	2020	0.7979	0.9794	0.9563	0.8227
Lv et al. [52].	2020	0.7941	0.9798	0.9558	0.8216
Sule et al. [53].	2020	0.7092	0.9820	0.9447	–
Li et al. [54].	2020	0.7735	0.9838	0.9673	0.8205
Zou et al. [55].	2021	0.7761	0.9792	0.9519	0.8129
Li et al. [56].	2021	0.7921	0.9810	0.9568	–
Proposed	2021	**0.7985**	0.9791	0.9561	**0.8229**

Table 5
The comparative results for different segmentation methods on STARE data set.

Method	Year	S_e	S_p	A_{cc}	F_1
Fraz et al. [38].	2012	0.7548	0.9763	0.9543	–
Liskowski et al. [41].	2016	0.7867	0.9754	0.9566	–
Orlando et al. [42].	2016	0.7680	0.9738	–	0.7644
Li et al. [39].	2016	0.7726	0.9844	0.9628	–
Zhang et al. [57].	2018	0.7673	**0.9901**	0.9712	–
Yan et al. [45].	2018	0.7581	0.9846	0.9612	–
Hu et al. [58].	2018	0.7543	0.9814	0.9632	–
Guo et al. [59].	2019	0.7548	0.9899	0.9725	–
Yan et al. [60].	2019	0.7735	0.9857	0.9638	–
Jin et al. [61].	2019	0.7595	0.9878	0.9641	0.8143
Lv et al. [52].	2020	0.7598	0.9878	0.9640	0.8142
Li et al. [54].	2020	0.7715	0.9886	0.9701	0.8146
Wu et al. [62].	2020	0.7963	0.9863	0.9672	–
Alvarado et al. [63].	2021	0.7904	0.9843	**0.9837**	0.8141
Yang et al. [64].	2021	0.7946	0.9821	0.9626	0.8155
Proposed	2021	**0.7963**	0.9792	0.9567	**0.8172**

Table 6
The comparative results for different segmentation methods on CHASE_DB1 data set.

Method	Year	S_e	S_p	A_{cc}	F_1
Ronneberger et al. [17].	2015	0.7841	0.9701	0.9578	0.7783
Li et al. [39].	2016	0.7507	0.9793	0.9581	–
Alom et al. [20].	2018	0.7756	0.9820	0.9634	0.7928
Yan et al. [45].	2018	0.7633	0.9809	0.9610	–
Zhuang et al. [44].	2018	0.7978	0.9818	0.9656	0.8031
Yan et al. [65].	2018	0.7633	0.9809	0.9610	–
Yan et al. [47].	2019	0.7641	0.9806	0.9607	–
Shin et al. [66].	2019	**0.9463**	0.9364	0.9373	–
Tang et al. [67].	2019	0.8106	0.9807	0.9654	–
Jin et al. [61].	2019	0.8155	0.9725	0.9610	0.7883
Lv et al. [52].	2020	0.8167	0.9704	0.9608	0.7892
Wang et al. [68].	2020	0.8239	0.9813	0.9670	0.8191
Li et al. [54].	2020	0.7970	0.9823	0.9655	0.8073
Wang et al. [69].	2020	0.7948	**0.9842**	0.9648	0.8220
Li et al. [56].	2021	0.7818	0.9819	0.9635	–
Yang et al. [70].	2020	0.8176	0.9776	0.9632	0.7997
Proposed	2021	0.8020	0.9794	**0.9672**	**0.8236**

of S_p and A_{cc} are not obvious. For the retinal vessel segmentation task, the fundus vessels always occupy a smaller pixel portion in retinal fundus images compared with background, which causes serious class imbalance issue. S_p measures the proportion of background pixels correctly identified, and A_{cc} is a comprehensive evaluation indicator for all prediction classes, which are easily affect by class imbalance issue.

Nevertheless, the correct identified vessel pixels are important for the segmentation task. S_e measures the proportion of retinal fundus vessels correctly identified. *Dice* evaluates the similarity of predictions and ground truth. These two evaluation indicators are not easily affected by foreground–background class imbalance issue. Due to the highest values of S_e and F_1 score on DRIVE, CHASE_DB1, and STARE sets, it could infer the effectiveness and superiority of the proposed segmentation network.

Due to higher S_e, it could be concluded that the proposed ResDO-UNet network could capture more vessels and details, but it also may introduce some noise, which leads to the over-segmentation phenomenon based on lower S_p and A_{cc}.

Meanwhile, the standard deviation on all test images for the mentioned three datasets is also calculated for an all-round experiment analysis, and Table 7 shows the experimental results of mean±standard deviation among these datasets.

As shown in Table 7, it could be seen that the standard deviation among these datasets has the small values, which could indicate the robustness and stability of proposed deep ResDO-UNet network. However, the standard deviation among these three datasets is different, and the standard deviation on DRIVE set is less than other two data sets, which is greatly affected by the presence of some lesion fundus images.

4.5. Qualitative analysis

To more intuitively observe the segmentation effect, the qualitative analysis is introduced into this paper for performance visualization. Based on the test sets in DRIVE set, CHASE_DB1 set, and STARE set, some sample images from test sets are selected as experimental objects, and Fig. 9 gives the corresponding segmentation results.

As shown in Fig. 9, the proposed ResDO-UNet network could achieved good segmentation results, and the blood vessels could be well detected from fundus images. From the probability maps, it can be seen that the proposed ResDO-UNet network could capture the details of blood vessels, but introduce some noise.

To realize better performance visualization of proposed ResDO-UNet network, some local details are provided for the qualitative analysis. Based on the cropped image paths, some challenging patches are selected for experimental analysis, and Fig. 10 shows the some patches and corresponding segmentation results.

With the qualitative results in Fig. 10, the image preprocessing has a certain filtering ability which could remove some interference, and the contrast between the blood vessels and background has got enhanced. Based on the above image patches, although the blood vessels have got well detected, there are still some over-segmentation areas due to similar texture to blood vessels. Meanwhile, because of low contrast, there are some under-segmentation areas in retinal fundus images.

In general, based on the above qualitative analysis and quantitative analysis, the proposed ResDO-UNet network could acquire a better segmentation performance on retinal fundus images.

5. Discussion

Accurate retinal vessel segmentation from fundus images plays the key role for the pathologic diagnosis of patients. However, the fundus images are always present some challenging factors, including weak texture of vessels, poor contrast, uneven illumination, complicated vessel structure, etc, which will bring a certain effect to accurate retinal vessel segmentation. Meanwhile, the class unbalance issue also will affect the whole segmentation performance.

Combined with effect context feature representation ability, DCNNs have shown a promising segmentation performance on medical images, including fundus images, especially the encoder–decoder framework. However, there are still some shortcomings on precise medical image segmentation, such as the information loss issue caused by multiple pooling operations and insufficient process issue of local context features by skip connections.

In this paper, to address the segmentation task, combined with the encoder–decoder framework, a novel deep ResDO-UNet network is proposed for automatic and accurate segmentation of retinal vessels from fundus images. It adopts the residual DO-conv network as backbone network to replace the original residual network which could acquire more effective contexts. On the basis, a PFB network is proposed to realize nonlinear fusion pooling to reduce the effect of the information loss issue caused by multiple pooling operations to the segmentation precision. Further, an AFB block is proposed for multi-scale feature representation, which could well address the insufficient process issue of local context features by skip connections. Meanwhile, it could well reduce the effect of semantic gap issue.

To better evaluate the segmentation performance of proposed ResDO-UNet network on fundus images, based on the quantitative analysis, the ablation study and comparison experiments are introduced for performance analysis. The ablation experiments have better clarify the effectiveness of proposed each network block to the whole segmentation performance, and the comparison experiments have proved the superiority of proposed segmentation network. Meanwhile, the qualitative analysis is also introduced for better performance visualization.

Combined with three public data sets on retinal vessel segmentation, the proposed ResDO-UNet network has proved a good segmentation performance on fundus images. For retinal vessel segmentation, both thick retinal vessels and thin retinal vessels are both key features for pathologic diagnosis of patients, and accurate thick retinal vessels and thin retinal vessels are both important for the segmentation task. However, these two retinal vessels have different signal-to-noise ratios, which will bring a certain challenge for accurate segmentation of thick retinal vessels and thin retinal vessels with a single-task segmentation model.

In the future, based on the present work, we will carry out the segmentation work with the multi-task learning scheme to further improve the segmentation performance on fundus images. Based on the different characteristics of these two retinal vessels, a multi-task learning model will be proposed to separately the thick retinal vessels and thin retinal vessels from the fundus images. And a feature fusion network is proposed to fuse the segmentation results from the multi-task learning model to improve the whole segmentation performance.

Table 7
Experiment results of mean±standard deviation on different datasets.

Dataset	S_e	S_p	A_{cc}	F_1
STARE	0.8039 ± 0.0296	0.9836 ± 0.0051	0.9635 ± 0.0037	0.8315 ± 0.0151
DRIVE	0.7985 ± 0.0109	0.9791 ± 0.0015	0.9561 ± 0.0015	0.8229 ± 0.0024
CHASE_DB1	0.8020 ± 0.0264	0.9794 ± 0.0021	0.9672 ± 0.0027	0.8236 ± 0.0161

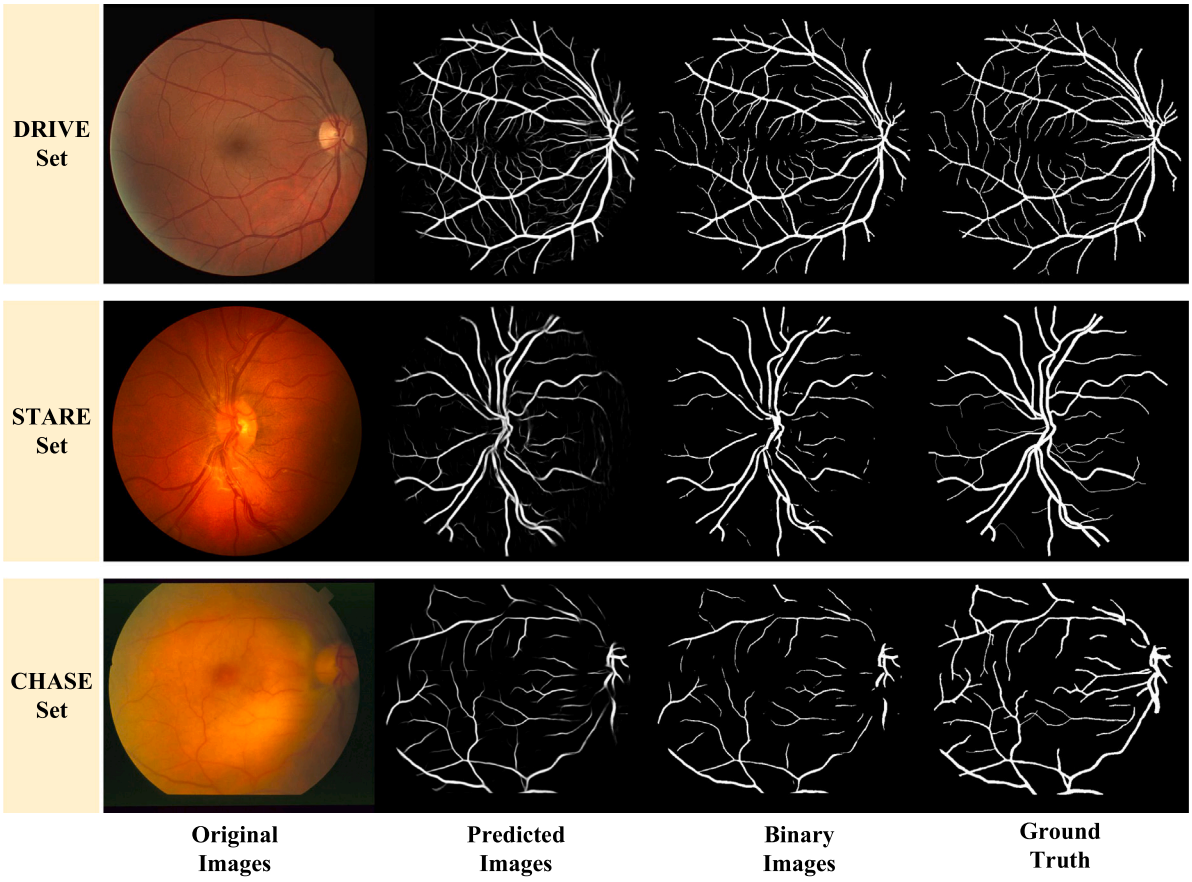

Fig. 9. Segmentation results of samples images.

6. Conclusion

Faced with the accurate segmentation task of retinal blood vessels, a novel deep ResDO-UNet network is proposed to provide an accurate and end-to-end detection scheme from fundus images. Experiments on multiple data sets about retinal image segmentation show that the proposed ResDO-UNet network could acquire a competitive segmentation performance compared with other advanced segmentation models. The main work of this paper is drawn as follows.

(1) A ResDO-conv network is proposed to realize strong context feature representation.

(2) To address information loss issue caused by multiple pooling operations, a PFB network block is proposed to realize nonlinear fusion pooling.

(3) Faced with insufficient process issue of local context features by skip connections, an AFB network block is proposed to realize effective multi-scale feature expression.

In the future work, we will focus on this research work to improve the segmentation performance on retinal vessels, to achieve a better segmentation effect.

CRediT authorship contribution statement

Yanhong Liu: Methodology, Writing – original draft. **Ji Shen:** Software, Validation. **Lei Yang:** Supervision, Resources, Visualization. **Guibin Bian:** Conceptualization, Methodology. **Hongnian Yu:** Writing – review & editing.

Declaration of competing interest

The authors declare that they have no known competing financial interests or personal relationships that could have appeared to influence the work reported in this paper.

Data availability

Data will be made available on request.

Acknowledgments

The authors wish to thank the anonymous reviewers for their valuable comments and suggestions.

This work was supported by the National Key Research & Development Project of China (2020YFB1313701), the National Natural Science Foundation of China (No. 62003309) and Outstanding Foreign Scientist Support Project in Henan Province of China (No. GZS2019008).

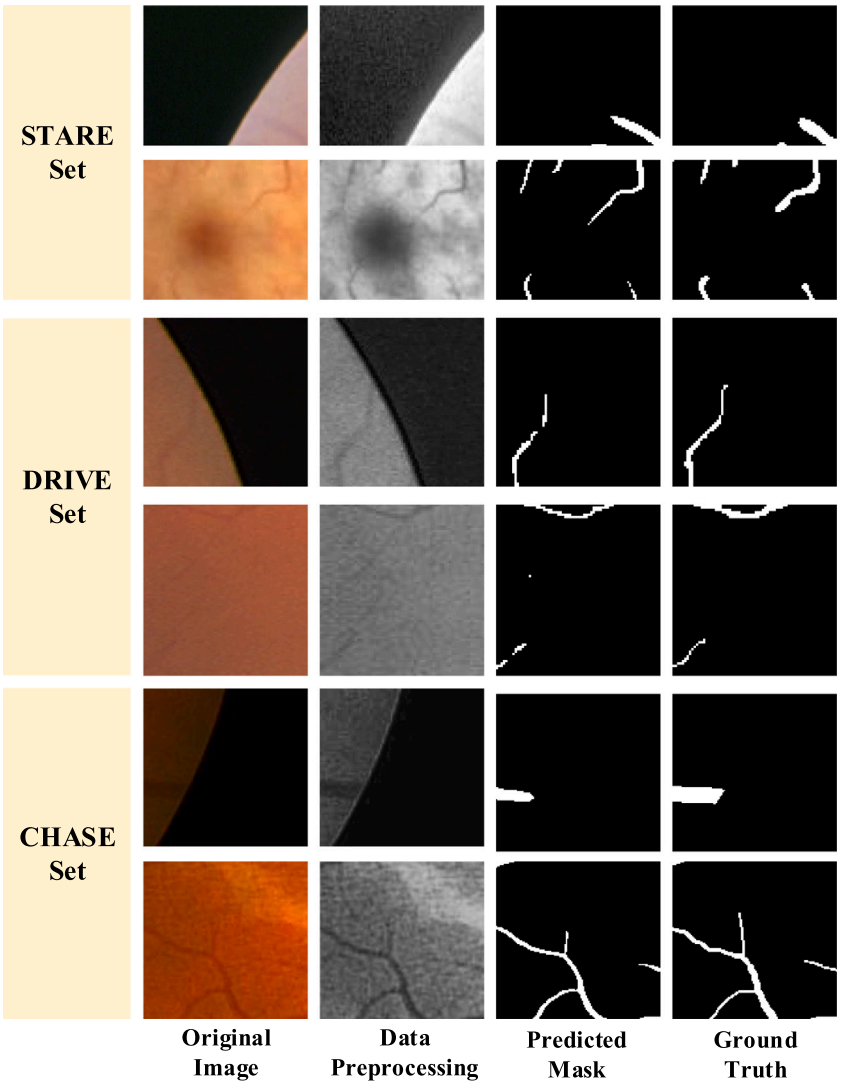

Fig. 10. Segmentation results of paths images.

References

[1] M. Li, Y. Yang, H. Jiang, G. Gregori, L. Roisman, F. Zheng, B. Ke, D. Qu, J. Wang, Retinal microvascular network and microcirculation assessments in high myopia, Am. J. Ophthalmol. 174 (2017) 56–67.

[2] I. Yilmaz, O.B. Ocak, B.S. Yilmaz, A. Inal, B. Gokyigit, M. Taskapili, Comparison of quantitative measurement of foveal avascular zone and macular vessel density in eyes of children with amblyopia and healthy controls: an optical coherence tomography angiography study, J. Am. Assoc. Pediatr. Ophthalmol. Strabismus 21 (3) (2017) 224–228.

[3] M. Bulut, F. Kurtuluş, O. Gözkaya, M.K. Erol, A. Cengiz, M. Akıdan, A. Yaman, Evaluation of optical coherence tomography angiographic findings in alzheimer's type dementia, Br. J. Ophthalmol. 102 (2) (2018) 233–237.

[4] J. Yu, K. Xiao, J. Huang, X. Sun, C. Jiang, Reduced retinal vessel density in obstructive sleep apnea syndrome patients: an optical coherence tomography angiography study, Invest. Ophthalmol. Vis. Sci. 58 (9) (2017) 3506–3512.

[5] A. Yarmohammadi, L.M. Zangwill, A. Diniz-Filho, M.H. Suh, S. Yousefi, L.J. Saunders, A. Belghith, P.I.C. Manalastas, F.A. Medeiros, R.N. Weinreb, Relationship between optical coherence tomography angiography vessel density and severity of visual field loss in glaucoma, Ophthalmology 123 (12) (2016) 2498–2508.

[6] L. Zhu, Y. Zong, J. Yu, C. Jiang, Y. He, Y. Jia, D. Huang, X. Sun, Reduced retinal vessel density in primary angle closure glaucoma: a quantitative study using optical coherence tomography angiography, J. Glaucoma 27 (4) (2018) 322.

[7] J.V. Soares, J.J. Leandro, R.M. Cesar, H.F. Jelinek, M.J. Cree, Retinal vessel segmentation using the 2-D Gabor wavelet and supervised classification, IEEE Trans. Med. Imaging 25 (9) (2006) 1214–1222.

[8] B. Zhang, L. Zhang, L. Zhang, F. Karray, Retinal vessel extraction by matched filter with first-order derivative of Gaussian, Comput. Biol. Med. 40 (4) (2010) 438–445.

[9] S. Roychowdhury, D.D. Koozekanani, K.K. Parhi, Blood vessel segmentation of fundus images by major vessel extraction and subimage classification, IEEE J. Biomed. Health Inf. 19 (3) (2014) 1118–1128.

[10] Y. LeCun, Y. Bengio, G. Hinton, Deep learning, Nature 521 (7553) (2015) 436–444.

[11] B. Zhao, J. Feng, X. Wu, S. Yan, A survey on deep learning-based fine-grained object classification and semantic segmentation, Int. J. Autom. Comput. 14 (2) (2017) 119–135.

[12] Z.-Q. Zhao, P. Zheng, S.-t. Xu, X. Wu, Object detection with deep learning: A review, IEEE Trans. Neural Netw. Learn. Syst. 30 (11) (2019) 3212–3232.

[13] D.D. Patil, S.G. Deore, Medical image segmentation: a review, Int. J. Comput. Sci. Mob. Comput. 2 (1) (2013) 22–27.

[14] J. Long, E. Shelhamer, T. Darrell, Fully convolutional networks for semantic segmentation, in: Proceedings of the IEEE Conference on Computer Vision and Pattern Recognition, CVPR, 2015, pp. 3431–3440.

[15] L.-C. Chen, G. Papandreou, F. Schroff, H. Adam, Rethinking atrous convolution for semantic image segmentation, 2017, arXiv preprint arXiv:1706.05587.

[16] V. Badrinarayanan, A. Kendall, R. Cipolla, Segnet: A deep convolutional encoder-decoder architecture for image segmentation, IEEE Trans. Pattern Anal. Mach. Intell. 39 (12) (2017) 2481–2495.

[17] O. Ronneberger, P. Fischer, T. Brox, U-net: Convolutional networks for biomedical image segmentation, in: Proceedings of International Conference on Medical Image Computing and Computer-Assisted Intervention, MICCAI, Springer, 2015, pp. 234–241.

[18] R. Mahum, S.U. Rehman, O.D. Okon, A. Alabrah, T. Meraj, H.T. Rauf, A novel hybrid approach based on deep CNN to detect glaucoma using fundus imaging, Electronics 11 (1) (2021) 26.

[19] S. Lal, S.U. Rehman, J.H. Shah, T. Meraj, H.T. Rauf, R. Damaševičius, M.A. Mohammed, K.H. Abdulkareem, Adversarial attack and defence through adversarial training and feature fusion for diabetic retinopathy recognition, Sensors 21 (11) (2021) 3922.
[20] M.Z. Alom, C. Yakopcic, M. Hasan, T.M. Taha, V.K. Asari, Recurrent residual U-Net for medical image segmentation, J. Med. Imaging 6 (1) (2019) 014006.
[21] C. Guo, M. Szemenyei, Y. Yi, W. Wang, B. Chen, C. Fan, Sa-unet: Spatial attention u-net for retinal vessel segmentation, in: Proceedings of 25th International Conference on Pattern Recognition, ICPR, IEEE, 2021, pp. 1236–1242.
[22] R. Azad, M. Asadi-Aghbolaghi, M. Fathy, S. Escalera, Bi-directional convlstm U-net with densley connected convolutions, in: Proceedings of the IEEE/CVF International Conference on Computer Vision Workshops, 2019.
[23] O. Oktay, J. Schlemper, L.L. Folgoc, M. Lee, M. Heinrich, K. Misawa, K. Mori, S. McDonagh, N.Y. Hammerla, B. Kainz, et al., Attention u-net: Learning where to look for the pancreas, 2018, arXiv preprint arXiv:1804.03999.
[24] M. Zhang, F. Yu, J. Zhao, L. Zhang, Q. Li, BEFD: Boundary enhancement and feature denoising for vessel segmentation, in: International Conference on Medical Image Computing and Computer-Assisted Intervention, Springer, 2020, pp. 775–785.
[25] L. Lin, J. Wu, P. Cheng, K. Wang, X. Tang, Blu-gan: Bi-directional convlstm u-net with generative adversarial training for retinal vessel segmentation, in: BenchCouncil International Federated Intelligent Computing and Block Chain Conferences, Springer, 2020, pp. 3–13.
[26] D. Lu, M. Heisler, D. Ma, S. Dabiri, S. Lee, G.W. Ding, M.V. Sarunic, M.F. Beg, Cascaded deep neural networks for retinal layer segmentation of optical coherence tomography with fluid presence, 2019, arXiv preprint arXiv:1912.03418.
[27] H. Li, J. Fang, S. Liu, X. Liang, X. Yang, Z. Mai, M.T. Van, T. Wang, Z. Chen, D. Ni, Cr-unet: A composite network for ovary and follicle segmentation in ultrasound images, IEEE J. Biomed. Health Inf. 24 (4) (2019) 974–983.
[28] L. Mou, Y. Zhao, H. Fu, Y. Liu, J. Cheng, Y. Zheng, P. Su, J. Yang, L. Chen, A.F. Frangi, et al., CS2-Net: Deep learning segmentation of curvilinear structures in medical imaging, Med. Image Anal. 67 (2021) 101874.
[29] K. O'Shea, R. Nash, An introduction to convolutional neural networks, 2015, arXiv preprint arXiv:1511.08458.
[30] J. Cao, Y. Li, M. Sun, Y. Chen, D. Lischinski, D. Cohen-Or, B. Chen, C. Tu, Do-conv: Depthwise over-parameterized convolutional layer, 2020, arXiv preprint arXiv:2006.12030.
[31] K. He, X. Zhang, S. Ren, J. Sun, Deep residual learning for image recognition, in: Proceedings of the IEEE Conference on Computer Vision and Pattern Recognition, CVPR, 2016, pp. 770–778.
[32] H. Gholamalinezhad, H. Khosravi, Pooling methods in deep neural networks, a review, 2020, arXiv preprint arXiv:2009.07485.
[33] C. Szegedy, V. Vanhoucke, S. Ioffe, J. Shlens, Z. Wojna, Rethinking the inception architecture for computer vision, in: Proceedings of the IEEE Conference on Computer Vision and Pattern Recognition, CVPR, 2016, pp. 2818–2826.
[34] L.-C. Chen, Y. Zhu, G. Papandreou, F. Schroff, H. Adam, Encoder-decoder with atrous separable convolution for semantic image segmentation, in: Proceedings of the European Conference on Computer Vision, ECCV, 2018, pp. 801–818.
[35] F. Yu, V. Koltun, Multi-scale context aggregation by dilated convolutions, 2015, arXiv preprint arXiv:1511.07122.
[36] J. Hu, L. Shen, G. Sun, Squeeze-and-excitation networks, in: Proceedings of the IEEE Conference on Computer Vision and Pattern Recognition, CVPR, 2018, pp. 7132–7141.
[37] J. Staal, M.D. Abràmoff, M. Niemeijer, M.A. Viergever, B. Van Ginneken, Ridge-based vessel segmentation in color images of the retina, IEEE Trans. Med. Imaging 23 (4) (2004) 501–509.
[38] M.M. Fraz, P. Remagnino, A. Hoppe, B. Uyyanonvara, A.R. Rudnicka, C.G. Owen, S.A. Barman, An ensemble classification-based approach applied to retinal blood vessel segmentation, IEEE Trans. Biomed. Eng. 59 (9) (2012) 2538–2548.
[39] Q. Li, B. Feng, L. Xie, P. Liang, H. Zhang, T. Wang, A cross-modality learning approach for vessel segmentation in retinal images, IEEE Trans. Med. Imaging 35 (1) (2015) 109–118.
[40] S. Roychowdhury, D.D. Koozekanani, K.K. Parhi, Blood vessel segmentation of fundus images by major vessel extraction and subimage classification, IEEE J. Biomed. Health Inf. 19 (3) (2014) 1118–1128.
[41] P. Liskowski, K. Krawiec, Segmenting retinal blood vessels with deep neural networks, IEEE Trans. Med. Imaging 35 (11) (2016) 2369–2380.
[42] J.I. Orlando, E. Prokofyeva, M.B. Blaschko, A discriminatively trained fully connected conditional random field model for blood vessel segmentation in fundus images, IEEE Trans. Biomed. Eng. 64 (1) (2016) 16–27.
[43] J. Mo, L. Zhang, Multi-level deep supervised networks for retinal vessel segmentation, Int. J. Comput. Assist. Radiol. Surg. 12 (12) (2017) 2181–2193.
[44] J. Zhuang, LadderNet: Multi-path networks based on U-Net for medical image segmentation, 2018, arXiv preprint arXiv:1810.07810.
[45] Z. Yan, X. Yang, K.-T. Cheng, Joint segment-level and pixel-wise losses for deep learning based retinal vessel segmentation, IEEE Trans. Biomed. Eng. 65 (9) (2018) 1912–1923.
[46] H. Xia, R. Zhuge, H. Li, Retinal vessel segmentation via a coarse-to-fine convolutional neural network, in: Proceedings of IEEE International Conference on Bioinformatics and Biomedicine, BIBM, IEEE, 2018, pp. 1036–1039.
[47] Z. Yan, X. Yang, K.-T. Cheng, A three-stage deep learning model for accurate retinal vessel segmentation, IEEE J. Biomed. Health Inf. 23 (4) (2018) 1427–1436.
[48] C. Guo, M. Szemenyei, Y. Pei, Y. Yi, W. Zhou, SD-Unet: a structured dropout u-net for retinal vessel segmentation, in: Proceedings of IEEE 19th International Conference on Bioinformatics and Bioengineering, BIBE, IEEE, 2019, pp. 439–444.
[49] A.P. Lopes, A. Ribeiro, C.A. Silva, Dilated convolutions in retinal blood vessels segmentation, in: Proceedings of IEEE 6th Portuguese Meeting on Bioengineering, ENBENG, IEEE, 2019, pp. 1–4.
[50] P. Yin, R. Yuan, Y. Cheng, Q. Wu, Deep guidance network for biomedical image segmentation, IEEE Access 8 (2020) 116106–116116.
[51] C. Chen, J.H. Chuah, A. Raza, Y. Wang, Retinal vessel segmentation using deep learning: A review, IEEE Access (2021).
[52] Y. Lv, H. Ma, J. Li, S. Liu, Attention guided u-net with atrous convolution for accurate retinal vessels segmentation, IEEE Access 8 (2020) 32826–32839.
[53] O. Sule, S. Viriri, Enhanced convolutional neural networks for segmentation of retinal blood vessel image, in: Proceedings of Information Communications Technology and Society, ICTAS, IEEE, 2020, pp. 1–6.
[54] L. Li, M. Verma, Y. Nakashima, H. Nagahara, R. Kawasaki, Iternet: Retinal image segmentation utilizing structural redundancy in vessel networks, in: Proceedings of the IEEE/CVF Winter Conference on Applications of Computer Vision, 2020, pp. 3656–3665.
[55] B. Zou, Y. Dai, Q. He, C. Zhu, G. Liu, Y. Su, R. Tang, Multi-label classification scheme based on local regression for retinal vessel segmentation, IEEE/ACM Trans. Comput. Biol. Bioinform. (2020).
[56] X. Li, Y. Jiang, M. Li, S. Yin, Lightweight attention convolutional neural network for retinal vessel image segmentation, IEEE Trans. Ind. Inf. 17 (3) (2020) 1958–1967.
[57] Y. Zhang, A.C. Chung, Deep supervision with additional labels for retinal vessel segmentation task, in: Proceedings of International Conference on Medical Image Computing and Computer-Assisted Intervention, MICCAI, Springer, 2018, pp. 83–91.
[58] K. Hu, Z. Zhang, X. Niu, Y. Zhang, C. Cao, F. Xiao, X. Gao, Retinal vessel segmentation of color fundus images using multiscale convolutional neural network with an improved cross-entropy loss function, Neurocomputing 309 (2018) 179–191.
[59] C. Guo, M. Szemenyei, Y. Pei, Y. Yi, W. Zhou, SD-UNet: A structured dropout U-Net for retinal vessel segmentation, in: Proceedings of IEEE 19th International Conference on Bioinformatics and Bioengineering, BIBE, IEEE, 2019, pp. 439–444.
[60] Z. Yan, X. Yang, K.-T. Cheng, A three-stage deep learning model for accurate retinal vessel segmentation, IEEE J. Biomed. Health Inf. 23 (4) (2018) 1427–1436.
[61] Q. Jin, Z. Meng, T. Pham, Q. Chen, L. Wei, R.D. Su, A deformable network for retinal vessel segmentation. arxiv 2018, 2020, arXiv preprint arXiv:1811.01206.
[62] Y. Wu, Y. Xia, Y. Song, Y. Zhang, W. Cai, NFN+: A novel network followed network for retinal vessel segmentation, Neural Netw. 126 (2020) 153–162.
[63] D.E. Alvarado-Carrillo, E. Ovalle-Magallanes, O.S. Dalmau-Cedeño, D-Gaussiannet: Adaptive distorted Gaussian matched filter with convolutional neural network for retinal vessel segmentation, Geom. Vis. 1386 (2021) 378.
[64] L. Yang, H. Wang, Q. Zeng, Y. Liu, G. Bian, A hybrid deep segmentation network for fundus vessels via deep-learning framework, Neurocomputing 448 (2021) 168–178.
[65] Z. Yan, X. Yang, K.-T. Cheng, Joint segment-level and pixel-wise losses for deep learning based retinal vessel segmentation, IEEE Trans. Biomed. Eng. 65 (9) (2018) 1912–1923.
[66] S.Y. Shin, S. Lee, I.D. Yun, K.M. Lee, Deep vessel segmentation by learning graphical connectivity, Med. Image Anal. 58 (2019) 101556.
[67] P. Tang, Q. Liang, X. Yan, D. Zhang, G. Coppola, W. Sun, Multi-proportion channel ensemble model for retinal vessel segmentation, Comput. Biol. Med. 111 (2019) 103352.
[68] D. Wang, A. Haytham, J. Pottenburgh, O. Saeedi, Y. Tao, Hard attention net for automatic retinal vessel segmentation, IEEE J. Biomed. Health Inf. 24 (12) (2020) 3384–3396.
[69] K. Wang, X. Zhang, S. Huang, Q. Wang, F. Chen, Ctf-net: Retinal vessel segmentation via deep coarse-to-fine supervision network, in: Proceedings of IEEE 17th International Symposium on Biomedical Imaging, ISBI, IEEE, 2020, pp. 1237–1241.
[70] L. Yang, H. Wang, Q. Zeng, Y. Liu, G. Bian, A hybrid deep segmentation network for fundus vessels via deep-learning framework, Neurocomputing 448 (2021) 168–178.